9. M. Sugitani, T. Sugai, M. Tanifuji, K. Murase, N. Onoda, *Neurosci. Lett.* **165**, 215 (1994); M. Sugitani, T. Sugai, M. Tanifuji, N. Onoda, *ibid.* **171**, 175 (1994).
10. VC slices (400 μm thick) were dissected from rats 4 to 8 weeks old [T. Kurotani, N. Yamamoto, K. Toyama, *Dev. Brain Res.* **71**, 151 (1993)] and were continuously superfused with Krebs-Ringer solution (control) consisting of 124 mM NaCl, 5.0 mM KCl, 1.24 mM KH_2PO_4, 2.0 mM $MgSO_4$, 2.0 mM $CaCl_2$, 26 mM $NaHCO_3$, and 10 mM glucose. The temperature was kept at 30°C throughout the experiment. Each slice was stained with a voltage-sensitive dye, RH482 (catalog no. NK3630, Nippon Kankoh-Shikiso Kenkyusho, Okayama, Japan) (at 0.1 mg/ml for 20 min), which is known to represent neural activity faithfully (*8*) [A. Konnerth, A. L. Obaid, B. M. Salzberg, *J. Physiol.* **393**, 681 (1987); M. Tanifuji, A. Yamanaka, K. Toyama, *Soc. Neurosci. Abstr.* **17**, 114 (1991)].
11. Stained slices were mounted on an inverted microscope (IMT-2, Olympus, Japan) that was equipped with a tungsten-halogen lamp (150 W), heat absorption (HA30, Kenko, Japan) and interference filters (700 ± 30 nm) (BPF-4, Vacuum Optics, Japan), a mechanical shutter, and an objective (PlanApo ×4, 0.2 numerical aperture, Nikon, Japan). The tungsten bipolar stimulation electrode (interpolar distance, 150 μm) was placed perpendicularly in the WM of a slice, where the cathode of the electrode was positioned on the border between WM and the gray matter. A glass electrode filled with 2% Pontamine sky blue and 0.85% NaCl (5 megohm) was placed in layer II-III to record field potentials. The length of illumination for the optical recording was minimized by the shutter (857 ms) to avoid dye bleaching and photodynamic damage. Stimulation was applied every 15 s. Stimulus intensity was adjusted to the strength that produced supramaximum responses of field potentials in layer II-III, which was in the range of 0.5 to 2.0 mA. Stimulus duration was 80 μs.
12. The field potential was continuously monitored throughout the experiment (peak amplitude, 1.57 ± 0.78 mV; latency, 10.01 ± 1.39 ms; $n = 27$), and no photodynamic effect on its amplitude and latency was observed by the optical recording.
13. The optical response evoked by stimulation of WM was recorded by a Fujix SD1001 (Fujifilm Microdevices, Japan). The recording system, consisting of a camera head with a 128 by 128 photodiode array and a processing unit that included digital frame memories, was based on a system designed by M. Ichikawa and colleagues [M. Ichikawa, T. Iijima, G. Matsumoto, in *Brain Mechanisms of Perception and Memory*, T. Ono, L. R. Squire, M. E. Raichle, D. I. Perrett, M. Fukuda, Eds. (Oxford Univ. Press, New York, 1993), pp. 638–648]. In each trial, a real-time image was taken about 500 ms before the stimulation and stored in one frame memory (reference image). Subsequent frames taken every 0.6 ms were subtracted from the reference image, amplified 400 times, and then stored in another frame memory (difference image). By this subtraction process, an accuracy (gray-level resolution) equivalent to 16-bit digitization was achieved. The difference image was usually averaged for 16 trials, and each frame was divided by a real-time image of the slice to express the optical responses as a percent of change in light absorption. Because of limited illumination by the shutter, this division process made no difference in the resulting image whether the real-time image used was taken before or after the optical recording ($n = 5$). Conventionally, the reference image taken at the last of 16 trials was used for division. The noise that accompanied the optical responses was due mainly to shot noise arising from the statistical noise of light. This noise was about 10 times smaller than the peak amplitude of the optical signals after averaging for 16 trials.
14. The time courses of the optical responses in each layer were reconstructed from serial frames. They consisted of rapidly rising and gradually recovering phases, which were similar to postsynaptic potentials in VC cells. The transient spiking responses were observed only around the cathode of the electrode and probably represented impulses evoked in the stimulated axons.
15. The horizontal spread was evaluated as being half the maximum width in a time-averaged response image constructed from serial frames of optical responses.
16. The cut was made with a fragment of a sharp razor blade held on a micromanipulator. The efficiency and exact position of the cut were examined by histology.
17. M. Tanifuji, T. Sugiyama, K. Murase, unpublished data.
18. The conduction velocity was calculated from the onsets of the optical responses along layers II-III and V (horizontal direction) and along a vertical line just above the stimulation electrode (vertical direction).
19. Y. Komatsu, S. Nakajima, K. Toyama, E. E. Fetz, *Brain Res.* **442**, 359 (1988); D. Ferster and S. Lindström, *J. Physiol.* **342**, 181 (1983).
20. U. Mitzdorf and W. Singer, *Exp. Brain Res.* **33**, 371 (1978).
21. J. A. Hirsch and C. D. Gilbert, *J. Neurosci.* **11**, 1800 (1991).
22. We thank Y. Komatsu, N. Yamamoto, and M. Crair for critical reading of the manuscript. Supported by Grants-in-Aid for Scientific Research Projects 05680695, 03260103, 04858070, and 06780531 from the Ministry of Education, Science, and Culture of Japan.

21 March 1994; accepted 20 September 1994

A Molecular Determinant for Submillisecond Desensitization in Glutamate Receptors

J. Mosbacher, R. Schoepfer, H. Monyer, N. Burnashev, P. H. Seeburg, J. P. Ruppersberg*

The decay of excitatory postsynaptic currents in central neurons mediated by α-amino-3-hydroxy-5-methyl-4-isoxazole-propionate (AMPA) receptors is likely to be shaped either by receptor desensitization or by offset after removal of glutamate from the synaptic cleft. Native AMPA receptors show desensitization time constants of 1 to about 10 milliseconds, but the underlying molecular determinants of these large differences are unknown. Cloned AMPA receptors carrying the "flop" splice variants of glutamate receptor subtype C (GluR-C) and GluR-D are shown to have desensitization time constants of around 1 millisecond, whereas those with the "flip" variants are about four times slower. Cerebellar granule cells switch their expression of GluR-D splice variants from mostly flip forms in early stages to predominantly flop forms in the adult rat brain. These findings suggest that rapid desensitization of AMPA receptors can be regulated by the expression and alternative splicing of GluR-D gene transcripts.

Native AMPA receptors have been studied in outside-out patches with rapid solution exchange techniques that allow agonist application times of less than 0.3 ms (*1*, *2*). These studies have allowed an estimate of the correlation between channel kinetics and the time course of synaptic events. Because data for the four cloned AMPA receptor subunits were obtained from whole-cell recordings (*3*–*6*) where the speed of agonist application is not faster than about 3 ms, current kinetics in the range between 1 and 3 ms will be underestimated. We therefore measured desensitization of different homo- and heterooligomeric AMPA receptors recombinantly expressed in *Xenopus laevis* oocytes in outside-out patches with a piezo-driven application technique (*1*, *7*, *8*).

J. Mosbacher and N. Burnashev, Max-Planck-Institut für medizinische Forschung, 69028 Heidelberg, Germany.
R. Schoepfer, Department of Pharmacology, Wellcome Laboratory of Molecular Pharmacology, University College London, Gower Street, London WC1E6BT, UK.
H. Monyer and P. H. Seeburg, Center for Molecular Biology, University of Heidelberg, 69120 Heidelberg, Germany.
J. P. Ruppersberg, Department of Sensory Biophysics, Ear, Nose, and Throat Hospital of the University of Tübingen, Röntgenweg 11, 72076 Tübingen, Germany.
*To whom correspondence should be addressed.

Homomeric AMPA receptor channels formed by the glutamate receptor D_{flop} (GluR-D_o) subunit desensitize four times faster than GluR-D_{flip} (GluR-D_i) channels (Fig. 1A and Table 1). The decay time constant of currents mediated by homomeric GluR-D_o channels in response to a 60-ms pulse of 1 mM glutamate (τ_{des}) was 0.9 ± 0.1 ms (mean ± SD). In contrast, for the splice variant GluR-D_i, which differs from the flop variant in only 11 amino acid residues (*3*), the corresponding value was 3.6 ± 0.6 ms. A similar difference in desensitization was found for GluR-C_o and GluR-C_i channels (Table 1). The occurrence of differences in desensitization time course is, however, not a general property of the splice variants for all four subunits. For GluR-A channels, there was no statistically significant difference between the flip-flop splice variants (Fig. 1B) (τ_{des} = 3.7 ± 0.7 ms for GluR-A_o and 3.4 ± 0.6 ms for GluR-A_i). GluR-B channels could not be measured in outside-out patches because of the small currents mediated by homooligomeric GluR-B channels.

We also investigated the current response to shorter glutamate pulses, where desensitization was incomplete and the offset after rapid removal of glutamate

could be measured. The difference in desensitization between the two GluR-D variants determines whether the decay phase of the currents depends on the duration of the glutamate application (Fig. 1C). Currents mediated by GluR-D_o were almost unchanged when the duration of glutamate pulses was increased stepwise from 1 to 8 ms. In contrast, the shape of GluR-D_i–mediated currents clearly depended on the duration of transmitter application. In GluR-D_o channels, desensitization was almost as fast as the offset (τ_{off} = 0.6 ± 0.1 ms, n = 7). Thus, the time course of removal of glutamate should not have a large influence on the time course of current decay. This is not the case for GluR-D_i, where desensitization is much slower than the offset of the current (τ_{off} = 0.6 ± 0.1 ms, n = 7). As for GluR-D, the flip-flop splice variants of GluR-A did not differ in the offset time constants even though these were significantly slower than for GluR-D [τ_{off} = 1.1 ± 0.2 ms for GluR-A_o (n = 9) and 1.1 ± 0.1 ms for GluR-A_i (n = 5)].

Many types of native neuronal AMPA receptors show only a small Ca^{2+} permeability, which is probably a result of the high expression levels of the edited form of the GluR-B subunit in the brain and its incorporation into heterooligomeric AMPA receptors (*4*, *9*–*12*). We therefore studied desensitization of flip-flop variants in heteromeric AMPA receptor channels containing the GluR-B subunit. The formation of heteromeric channels was verified by the shape of their current-voltage (*I-V*) relation. Heteromeric channels containing the GluR-B subunit have a more linear *I-V* relation than homomeric GluR-A, -C, and -D channels have (Fig. 2B). This *I-V* relation is not a superimposition of the *I-V* values of the homomeric channels because of the small currents mediated by homomeric GluR-B channels. The GluR-D subunit variants also determined the desensitization time course of GluR-B or -D heteromeric channels (Fig. 2A and Table 1) in the same way as observed for the GluR-D homomeric channels (Fig. 1, A and C). Similarly, heterooligomers containing the GluR-C subunit showed a difference in their speed of desensitization, which was less pronounced than the difference between the GluR-D subunits (Table 1). The influence of the splice variants of GluR-B in heterooligomers was significant but weaker than for GluR-C and -D channels (Table 1). Similar to the behavior of homooligomeric GluR-A channels, the splice variants of the GluR-A subunit coexpressed with GluR-B showed no detectable differences in their time constants (Table 1). However, even with a similar time course of desensitization, subunit combinations containing the flip or flop variants of GluR-A differed in the ratio of their peak current (I_{peak}) to steady-state current (I_{ss}), which can explain the difference of steady-state components shown (*3*): I_{peak}/I_{ss}(GluR-A_i/B_i) = 108 ± 26 (mean ± SEM; n = 23) and I_{peak}/I_{ss}(GluR-A_o/B_i) = 237 ± 33 (n = 18). These results indicate that the influence of flip-flop splice variants on desensitization is specific to each subunit and is strongest for the GluR-C and, particularly, the GluR-D subunits.

Besides desensitization, the flip and flop modules also influenced the rise time of the currents (the current rise from 20 to 80% of the peak was 0.53 ms for GluR-B_i/D_i channels but was only 0.18 ms for GluR-B_o/D_o channels) (Fig. 2C). However, this could also be explained by the different desensitization time courses with identical activation time constants, assuming that desensitization starts immediately with glutamate application. Results consistent with this hypothesis are shown in Fig. 2C, where currents are scaled with respect to the maximal slope of their rising phase. This scaling resulted in all four fits to the desensitization phase crossing almost at the same point at the beginning of glutamate application. Hence, it seems likely that the activation rate is approximately the same for the different combinations but that the rising phase is cut at different time points, depending on desensitization rate. Although how far desensitization contributes to the decay phase of excitatory postsynaptic currents (*1*, *13*–*19*) is still under discussion, the decay rate of currents mediated by AMPA receptors containing GluR-C_o or -D_o subunits cannot be slower than their desensitization rate, even though glutamate may still be present in the synaptic cleft.

In situ hybridization (*9*, *20*, *21*) and

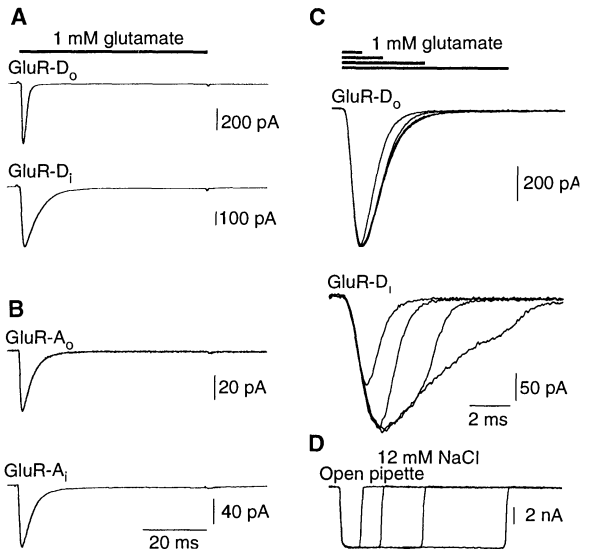

Fig. 1. Currents mediated by recombinant homomeric AMPA receptor channels differ in their time course of desensitization. (**A**) GluR-D_o channels desensitize four times faster in response to a 60-ms glutamate pulse (1 mM) at −40 mV than GluR-D_i channels. (**B**) GluR-A_o and GluR-A_i channels show no significant difference in desensitization [same conditions as in (A)]. In (A) and (B), averages of 10 to 40 single responses to glutamate application are displayed. (**C**) Responses of GluR-D_o and GluR-D_i channels as in (A) but to short glutamate pulses of 1, 2, 4, and 8 ms in duration. (**D**) Estimated time course of application. After disrupting the patch, we switched the open pipette between normal and 10× diluted NFR solution (*8*). Solution exchange could be achieved in less than 100 μs (20 to 80%) with our fast application system. The desensitization time constants of currents mediated by GluR-D_i and GluR-D_o showed no large concentration dependence. For 0.3 and 3 mM glutamate, τ_{des} was 4.2 ± 0.1 ms and 3.8 ± 0.5 ms (n = 3) for GluR-D_i, and 0.9 ± 0.2 ms and 0.7 ± 0.2 ms (n = 3) for GluR-D_o, respectively.

Table 1. Desensitization time constants of all AMPA receptor subunit combinations investigated. Values were obtained by monoexponential fits to the decay phase of the currents and are given in milliseconds (mean ± standard deviation); the number of patches is in parentheses. Desensitization was tested independently in a different expression system (HEK293 cells) (*28*) but also with outside-out patches and fast glutamate application. Here, only the highly expressing combination GluR-A_i/B_i could be tested, and in two experiments desensitization time constants of 4.2 and 4.9 ms were obtained. These values were within the range of those obtained in patches from *Xenopus* oocytes, indicating the absence of system-specific differences.

Channel type	Desensitization time constants for glutamate receptor subunit					
	A_{flip}	A_{flop}	C_{flip}	C_{flop}	D_{flip}	D_{flop}
Homomeric channels	3.4 ± 0.6 (11)	3.7 ± 0.7 (17)	4.8 ± 0.6 (8)	1.4 ± 0.4 (8)	3.6 ± 0.6 (10)	0.9 ± 0.1 (19)
Combinations with GluR-B_{flip}	5.1 ± 0.9 (27)	5.2 ± 0.8 (20)	4.9 ± 1.1 (14)	2.3 ± 0.6 (12)	6.1 ± 1.5 (23)	1.1 ± 0.2 (15)
Combinations with GluR-B_{flop}	3.4 ± 0.4 (8)	2.8 ± 0.4 (21)	2.9 ± 0.5 (6)	1.1 ± 0.2 (3)	3.7 ± 1.0 (17)	0.8 ± 0.1 (8)

single-cell polymerase chain reaction experiments (*12*, *22*, *23*) have shown tissue-specific and developmentally regulated expression of AMPA receptor splice variants. Figure 3 shows the developmentally controlled switch of GluR-D transcript splicing in cerebellar granule cells. In rats younger than 9 days, little GluR-D_o is expressed, but GluR-D_i mRNA is prominent in the granule cell layer. AMPA receptors studied in cultures of granule cells from 6-day-old rats show a desensitization time constant of about 3 ms (*24*). By postnatal day 9, amounts of GluR-D_o mRNA have increased and appear to correlate with fast synaptic transmission, with decay time constants of about 1 ms observed in cerebellar granule cells at this age (*25*). Fast synaptic transmission and submillisecond desensitization have also been detected in other parts in the brain—for example, in cells of the cochlear nucleus (*2*, *16*, *26*). Our results emphasize the importance of splice variant–specific expression and support the hypothesis that alternative splicing can change AMPA receptor channel kinetics, which influences the shape of synaptic currents.

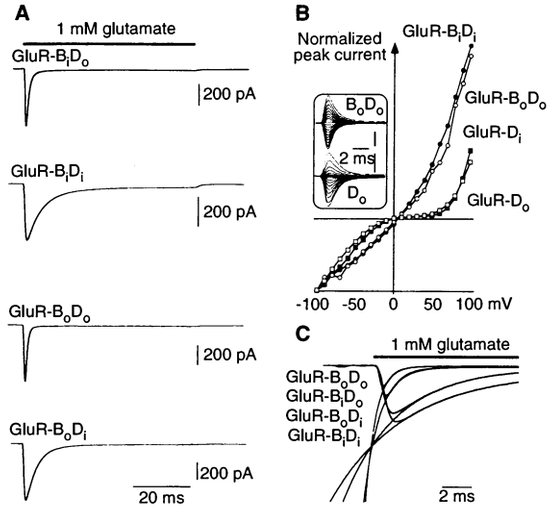

Fig. 2. Desensitization of heteromeric AMPA receptors containing the GluR-B subunit. (**A**) AMPA receptors formed upon co-injection into *Xenopus* oocytes of equal amounts of GluR-D– and GluR-B–specific cRNAs were fast desensitizing if GluR-D was in the flop form. The flip and flop variants of the GluR-B subunit had less influence on the time course of desensitization. (**B**) Difference between the *I-V* relations of homomeric and GluR-B–containing heteromeric channels. Peak *I-V* relations were obtained from three averaged responses to 60-ms glutamate pulses as in (A) at test potentials from −100 to +100 mV in 10-mV increments as shown in the inset. Scale bars in the inset are 500 pA for GluR-B_o/D_o and 200 pA for GluR-D_o. Heteromeric channels containing GluR-B showed a more linear *I-V* relation of their peak currents, whereas homomeric GluR-D as well as GluR-A and GluR-C (not shown) channels showed inward and outward rectification. These results are similar to those found for the steady-state current in transfected cells (*28*). Desensitization time constants showed a small voltage dependence [GluR-B_o/D_o: τ_{des} (−100 mV) = 0.9 ms, τ_{des} (+100 mV) = 1.2 ms; GluR-D_o: τ_{des} (−100 mV) = 0.9 ms, τ_{des} (+100 mV) = 1.3 ms; these data are from traces shown in the inset]. (**C**) Current traces from (A) but scaled with respect to their maximal slope of the activation phase (numerically calculated as the minimum of the first derivative), so that the rising phases overlap maximally. Halftone traces represent monoexponential fits to the decays of the currents obtained in a fitting range from the inflection point after the peak to the point measured about 40 ms after the peak.

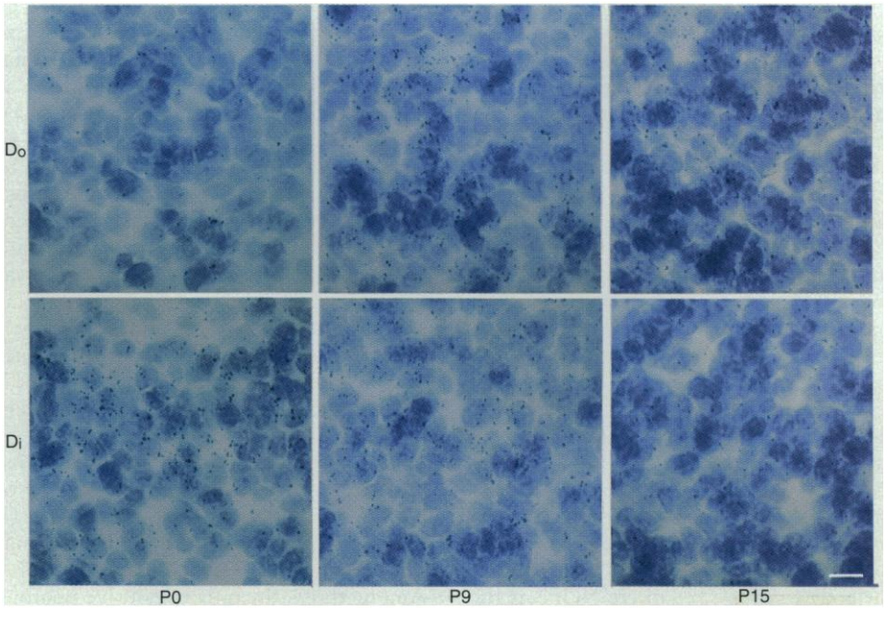

Fig. 3. Developmentally regulated expression of GluR-D_i and GluR-D_o in cerebellar granule cells. Shown are in situ hybridizations with oligonucleotides specific to GluR-D_i and GluR-D_o mRNA (*20*) at cellular resolution in cerebellar granule cells of postnatal day 0 (P0), P9, and P15 rat brains. Bar, 25 mm. All panels show representative hybridization intensities as found for the cerebellar granule cell layer of each respective age.

REFERENCES AND NOTES

1. D. Colquhoun, P. Jonas, B. Sakmann, *J. Physiol. (London)* **458**, 261 (1992).
2. I. M. Raman and L. O. Trussel, *Neuron* **9**, 173 (1992).
3. B. Sommer *et al.*, *Science* **249**, 1580 (1990).
4. T. A. Verdoorn, N. Burnashev, H. Monyer, P. H. Seeburg, B. Sakmann, *ibid.* **252**, 1715 (1991).
5. R. I. Hume, R. Dingledine, S. F. Heinemann, *ibid.* **253**, 1028 (1991).
6. N. Burnashev, *Cell Physiol. Biochem.* **3**, 318 (1993).
7. J. Dudel, C. Franke, H. Hatt, *Neurosci. Lett.* **77**, 199 (1987).
8. A/MPA receptor–specific complementary RNA (cRNA) was synthesized and injected into *X. laevis* oocytes as described (*27*). For heteromultimeric receptors, equal volumes of dissolved cRNA (about 1 μg/μl) were injected. Three to seven days after injection, outside-out patches were isolated from oocytes and exposed to a piezo-controlled fast application system with a double-barrel application pipette. For fast application, we used normal frog Ringer solution (NFR) containing 115 mM NaCl, 2.5 mM KCl, 1.8 mM $CaCl_2$, and 10 mM Hepes (pH 7.2; NaOH), where 1 mM glutamate was added to the test solution. The patch pipettes were pulled from thick-wall borosilicate glass, were filled with a solution containing 100 mM KCl, 2 mM $MgCl_2$, 10 mM EGTA, and 10 mM Hepes (pH 7.2; KOH), and had a tip resistance of 3 to 5 megohms. All experiments were done at an ambient temperature of about 23°C and at a holding potential of −40 mV. Currents were filtered at 5 to 10 kHz and digitized at 15 kHz. We obtained desensitization and offset time constants by fitting a single exponential function to the decay of current evoked by a 60-ms and a 1-ms glutamate pulse, respectively.
9. B. Sommer, M. Köhler, R. Sprengel, P. H. Seeburg, *Cell* **67**, 11 (1991).
10. M. Hollmann, M. Hartley, S. Heinemann, *Science* **252**, 851 (1991).
11. N. Burnashev *et al.*, *ibid.* **256**, 1566 (1992).
12. P. Jonas, C. Racca, B. Sakmann, P. Seeburg, H. Monyer, *Neuron* **12**, 1281 (1994).
13. L. O. Trussell and G. D. Fischbach, *ibid.* **3**, 209 (1989).
14. L. Vyklicky Jr., D. K. Patneau, M. L. Mayer, *ibid.* **7**, 971 (1991).
15. S. Hestrin, *ibid.* **9**, 991 (1992).
16. L. O. Trussel, S. Zhang, I. M. Raman, *ibid.* **10**, 1185 (1993).
17. S. Hestrin, *ibid.* **11**, 1083 (1993).
18. P. Jonas and B. Sakmann, *J. Physiol. (London)* **455**, 143 (1992).
19. B. Barbour, B. U. Keller, I. Llano, A. Marty, *Neuron* **12**, 1331 (1994).
20. H. Monyer, P. H. Seeburg, W. Wisden, *ibid.* **6**, 799 (1991).
21. V. Gallo *et al.*, *J. Neurosci.* **12**, 1010 (1992).
22. B. Lambolez, E. Audinat, P. Bochet, F. Crepel, J. Rossier, *Neuron* **9**, 247 (1992).
23. P. Bochet *et al.*, *ibid.* **12**, 383 (1994).
24. B. Edmonds, R. A. Silver, D. Colquhoun, S. G. Cull-Candy, *Soc. Neurosci. Abstr.* **19**, 1515 (1993).

25. R. A. Silver, S. F. Traynelis, S. G. Cull-Candy, *Nature* **355**, 163 (1992).
26. J. T. Hackett, H. Jackson, E. W. Rubel, *Neuroscience* **7**, 1455 (1982).
27. S. Herlitze *et al.*, *Neuron* **10**, 1131 (1993).
28. N. Burnashev, H. Monyer, P. H. Seeburg, B. Sakmann, *ibid.* **8**, 189 (1992).

29. We thank B. Sakmann and H. Ehmke for advice and helpful discussions; W. Günther and T. Kuner for synthesis of cRNA; M. Kaiser, U. Keller, H. Hörber, and K. Bauer for technical support; and B. Fakler and L. Wollmuth for critically reading the manuscript.

28 July 1994; accepted 13 September 1994

GDNF: A Potent Survival Factor for Motoneurons Present in Peripheral Nerve and Muscle

Christopher E. Henderson, Heidi S. Phillips, Richard A. Pollock, Alun M. Davies, Corinne Lemeulle, Mark Armanini, Lora C. Simpson, Barbara Moffet, Richard A. Vandlen, Vassilis E. Koliatsos,* Arnon Rosenthal*†

For survival, embryonic motoneurons in vertebrates depend on as yet undefined neurotrophic factors present in the limb bud. Members of the neurotrophin family are currently the best candidates for such neurotrophic factors, but inactivation of their receptor genes leads to only partial loss of motoneurons, which suggests that other factors are involved. Glial cell line–derived neurotrophic factor (GDNF), originally identified as a trophic factor specific for dopaminergic neurons, was found to be 75-fold more potent than the neurotrophins in supporting the survival of purified embryonic rat motoneurons in culture. GDNF messenger RNA was found in the immediate vicinity of motoneurons during the period of cell death in development. In vivo, GDNF rescues and prevents the atrophy of facial motoneurons that have been deprived of target-derived survival factors by axotomy. GDNF may therefore be a physiological trophic factor for spinal motoneurons. Its potency and specificity in vitro and in vivo also make it a good candidate for treatment of motoneuron disease.

The survival of developing motoneurons depends on trophic factors derived from their target, the limb bud, and from in the central nervous system (*1*). The best candidates for physiological motoneuron trophic factors are currently the neurotrophins brain-derived neurotrophic factor (BDNF), neurotrophin-3 (NT-3), and neurotrophin-4/5 (NT-4/5): These molecules are the most potent survival factors known for motoneurons in vitro and in vivo, are expressed in muscle during naturally occurring motoneuron cell death, and can be retrogradely transported by motoneurons (*2–4*). Moreover, mice in which TrkB and TrkC (the high-affinity receptors for these factors) are inactivated show a 30% loss of spinal motoneurons and 70% loss of facial motoneurons (*5*) at the end of fetal development, which suggests that at least a subpopulation of motoneurons requires neurotrophins to survive. However, the incomplete motoneuron loss in the null-mutant mice suggests that some motoneurons have access to other survival-promoting molecules. We therefore searched for additional factors that might act specifically on motoneurons. GDNF, a distant member of the transforming growth factor–β family, was recently purified from the supernatant of the B49 glial cell line. It has potent effects on the survival and maturation of cultured dopaminergic neurons from rat embryonic midbrain and is expressed in the embryonic striatum and other neuronal structures (*6*).

To determine the effect of GDNF on motoneurons, we prepared enriched cultures from embryonic day 14 (E14) rat spinal cord by a combination of metrizamide density gradient centrifugation and "immunopanning" (adhesion to plates coated with antibodies) with a specific antibody to $p75^{NGFR}$ (where NGFR is the nerve growth factor receptor) (*4*, *7*). In these cultures, 93 ± 3% (mean ± SEM; n = 4) of the cells were typical motoneurons. They were large and multipolar and were stained by antibodies to the motoneuron-specific homeoprotein Islet-1 (*8*) (Fig. 1A). The remaining cells (~7%) were smaller, did not stain for Islet-1, and were excluded from the cell counts. As reported (*4*, *9*), a subpopulation of Islet-1–positive motoneurons (33.4 ± 0.6%; n = 5) does not require trophic support other than that provided by basal culture medium. However, most motoneurons (~67%) are dependent on trophic factors and require muscle extract for survival (*4*). We tested the ability of recombinant rat GDNF to support the muscle-dependent motoneuron population. Purified motoneurons were seeded at low density in the presence of serial dilutions of GDNF (Fig. 1B). After 55 hours in culture, motoneuron survival increased in a dose-dependent manner with a median effective concentration (EC_{50}) of 0.2 ± 0.1 pg/ml (n = 3), equivalent to 7 fM GDNF dimer. Concentrations above 10 pg/ml were saturating, and 88.8 ± 4.1% (n = 4) of viable motoneurons were maintained (*10*).

We compared the potency of GDNF to that of other factors with motoneuron survival activity. Dose-response analysis demonstrated that in this in vitro assay, GDNF is 75-, 650-, and 2500-fold more potent than recombinant rat BDNF, rat ciliary neurotrophic factor (CNTF), and human cholinergic differentiation factor–leukemia inhibitory factor (CDF-LIF), respectively. The EC_{50} values for the other factors (BDNF, CNTF, and CDF-LIF) were similar to those reported (*4*, *9*, *11*); the rank order of potency presented here is thus not a function of the culture system used. GDNF also had the highest efficacy in supporting motoneuron survival. Expressed relative to the value of the optimal concentration of BDNF (defined as 100%), GDNF caused 115 ± 8% (n = 5), CNTF 51 ± 7% (n = 4), and CDF-LIF 44 ± 6% (n = 4) of the motoneurons to survive. Furthermore, no additive effect was apparent, even when all factors were combined. These findings demonstrate that GDNF is the most potent survival factor for motoneurons identified so far and suggest that GDNF and BDNF each support essentially all motoneurons purified by immunopanning, whereas CNTF and CDF-LIF act on only approximately half of the same population (*9*, *11*).

In contrast to the neurotrophins, GDNF had no effect on the survival of peripheral sensory neurons from the E15 nodose, E15 trigeminal, or E18 trigeminal ganglia or of E18 sympathetic neurons. Among those, the only responsive neurons were from a subpopulation of the E18 nodose neurons that also respond to BDNF (Table 1). The neurotrophic effects of GDNF at the periphery are therefore specific.

C. E. Henderson, R. A. Pollock, C. Lemeulle, INSERM U.382, IBDM, Case 907 Luminy, 13288 Marseille Cedex 9, France.
H. S. Phillips, M. Armanini, L. C. Simpson, B. Moffet, R. A. Vandlen, A. Rosenthal, Departments of Neuroscience, Protein Chemistry, and Cell Genetics, Genentech, South San Francisco, CA 94080–4990, USA.
A. M. Davies, School of Biological and Medical Sciences, St. Andrews, Scotland.
V. E. Koliatsos, Department of Pathology, Neurology, and Neuroscience and Neuropathology Laboratory, Johns Hopkins University School of Medicine, Baltimore, MD 21205, USA.

*The last two authors made equal contributions to the manuscript.
†To whom correspondence should be addressed.